

Conservative numerical methods for simulation of heat-shield degradation during hypersonic re-entry

Alexis Cas¹, Céline Baranger², Héloïse Beaugendre³, Simon Peluchon⁴

Abstract

During atmospheric hypersonic re-entry, the heat distribution within the thermal protection system (TPS) is dampened by the in-depth chemical degradation of materials - called pyrolysis -, and by a surface physico-chemical degradation - called ablation. The aim of this work is to investigate the numerical tools used to solve the thermal pyrolysis response of heat shield. First, an overview of macroscopic modeling of pyrolysis will be done. Arrhenius laws are employed in the modeling of density variation. Swelling or shrinkage are taken into account as a consequence of material degradation. This analysis will explore a number of numerical methods, with a focus on conservation properties and method efficiency. Finally, Henderson's experimental test case is studied, in order to validate and compare the numerical methods. The simulation results are in reasonable agreement with the experimental data. Some numerical methods result in a trade-off between mass or energy conservation and a faster computation time.

Keywords: Pyrolysis model, Conservation laws, Numerical resolution, Domain deformations

1. Introduction

The thermal protection system provides effective vehicle interior safety during atmospheric hypersonic re-entry, sacrificing itself. Extreme conditions greatly damage the shield, which is designed to lower the temperature through chemical decomposition due to pyrolysis and surface degradation due to ablation.

Pyrolysis models have been numerous since the first mathematical model of pyrolysis, developed by Bamford in 1946 [2]. Pyrolysis reactions are modeled by reactions following Arrhenius laws. Models have been developed in three communities: biomass, atmospheric re-entry and combustion. By studying the three communities, Lachaud [11] concluded that there were three levels of pyrolysis modeling. The first level of pyrolysis modeling simplifies the description of pyrolysis gases, without using its properties and without computing its direction and pressure. Krastch introduced these models into the reentry field [9]. Subsequently, CMA [13] and FIAT [4] were implemented. The second type of model improves gas modeling using Darcy's law, determining the velocity and direction of pyrolysis gases. More detailed microscopic models, using the equilibrium or finite-rate chemistry models [11], were then developed, described as the third level of modeling. Finally, it should be pointed out that another type of model has also been developed, no longer using parallel independent reactions, but instead involving competitive reactions [15]. Besides, thermal expansion and deformations due to material heating and chemical degradation have been considered. First, expansion was computed based on empirical relationship, according to mass loss [1], temperature and mass variations [8] or gases trapped [14]. More recent developments model the mechanical part of the solid in order to compute stress, strain and deformations [12].

The presented model is based on the first level of pyrolysis modeling, with gases following a specific directional flow, constrained by material manufacturing, due to the low level of porosity of the TPS. The

¹CEA-CESTA, 15 Av. des Sablières, 33114 Le Barp, France, alexis.cas@cea.fr

²CEA-CESTA, 15 Av. des Sablières, 33114 Le Barp, France, celine.baranger@cea.fr

³Institut de Mathématiques de Bordeaux (IMB), Université de Bordeaux, CNRS UMR 5251, Bordeaux INP, INRIA, F-33400, Talence, France, heloise.beaugendre@math.u-bordeaux.fr

⁴CEA-CESTA, 15 Av. des Sablières, 33114 Le Barp, France, simon.peluchon@cea.fr

pyrolysis resolution can be done using several parallel Arrhenius laws [5], but will be presented below using a single Arrhenius law, for simplicity's sake. The deformations of the domain are modeled from a macroscopic point of view, using Henderson's empirical law [8]. The first contribution of this work is to assess how the numerical resolution of the pyrolysis model affects the mass and energy conservation. The second contribution lies in proposing a new approach to the original model, by adjusting virgin and char density according to the domain deformations.

2. Thermal response model

2.1. Physical context

During the pyrolysis process of a solid, subjected to a high heat flux, several degradation stages can be outlined. The virgin material heats up promptly through conduction, leading to its drying. Following the drying phase, a zone of chemical decomposition, known as pyrolysis, forms as a result of various chemical reactions. Pyrolysis leads to a loss of solid mass. This process ultimately gives rise to charred material. Throughout this degradation process, the properties of the material, such as density, conductivity, porosity, permeability, and specific heat capacity are altered significantly. At the same time, pyrolysis gases are generated within the pyrolysis zone, becoming trapped in the charred material's pores, resulting in material swelling. The release of the gases and the drying out of the material lead to shrinkage. Moreover, thermal expansion can be experienced throughout the heating process. The escaped pyrolysis gases interact with each other and with the degraded material, removing energy through convection. These effects contribute to cracking and coking within the solid. As a result of strong heat flux imposed on the wall, the solid may also undergo a wall recession called ablation. A simplified description of the decomposition process is displayed in Figure 1.

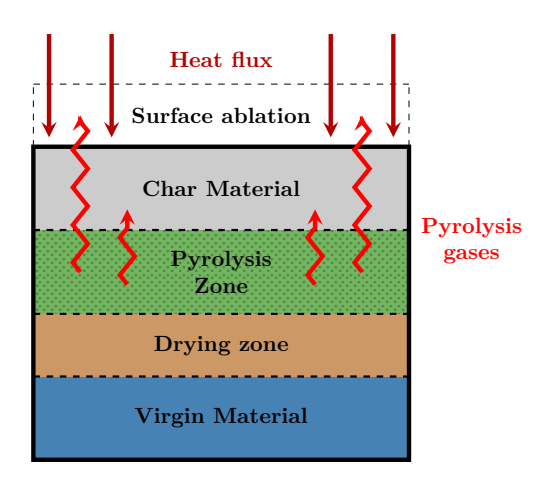


Fig 1. Pyrolysis phenomenon.

The physical model employed is a simplified macroscopic model that does not account for chemical reactions. Three zones of the solid are taken into account: the virgin zone, the pyrolyzed zone and the char zone. The solid is considered to lack porosity. Thus, pyrolysis gases are included in the model but are expelled toward the boundary layer along the material's manufacturing directions. Thermal equilibrium is considered, which means that the gas temperature is the same as the solid temperature. Macroscopic deformations, such as thermal expansion, swelling or shrinkage, are taken into account, while internal stresses are not considered. Drying and cracking of the solid are taken into account via the thermal properties of the material. Finally, a simplified mathematical model will be presented, where the variations in gas density and porosity will be very slight and therefore negligible.

2.2. Mathematical model

The system studied is a solid during atmospheric re-entry, which may be porous, composed of pyrolysable (e.g. resin) and non-pyrolysable materials (e.g. carbon fiber). Under the effect of high temperatures and high heating rates, the solid will undergo in-depth chemical degradation. The degradation of pyrolysable

materials will release pyrolysis gases and will produce carbonized material as described in section 2.1. Therefore, the system will be formed of the solid, composed of several materials (pyrolysable or not), and several pyrolysis gases. Each pyrolysable material will undergo a single pyrolysis reaction, dampening its mass and releasing a specific gas. In contrast, non-pyrolysable materials will not release gas, and their mass will remain constant. The solid may undergo small deformations such as swelling and shrinkage. These deformations would alter the density of each material, even if the material does not pyrolyze, as volume evolves, in order to satisfy the mass conservation. Therefore, the model employed allows the virgin and the char density to fluctuate. Given the characteristic times for the solid thermal response and solid deformations, the resolution of the thermal properties and the deformations can be split. First, thermal properties are determined through the mass and energy conservation equations of the solid and the gas. Then, steady state domain deformations are determined using a simplified model and the updated properties.

The studied domain $\Omega(t)$ consists of a solid and its pyrolysis gases, with a total density ρ and a total mass m. Solid properties are denoted with a superscript s, and gas properties with a superscript g. The pyrolysable solid undergoes degradation from surface heat flux, causing a loss in mass. Thus, if the solid is able to pyrolyze, a destruction term, the pyrolysis function noted Π_m , has to be added to the mass conservation equation. Hence, the solid mass conservation equation of the system is stated as follows:

$$\frac{dm^s}{dt} = -\Pi_m, \text{ on } \Omega(t). \tag{1}$$

The decomposition function Π_m can be computed using several Arrhenius laws, computed in parallel [5]. For convenience, the one-law model will be presented.

$$\Pi_m = Am_v \left(\frac{m^s - m_c}{m_v}\right)^{Na} \exp^{-\frac{T_a}{T}}.$$
 (2)

Where A is the pre-exponential factor and T_a is the activation temperature of the Arrhenius law of order Na. These coefficients are obtained using thermogravimetric analysis (TGA) data. The subscript v refers to the virgin material and the subscript c refers to the charred material. The idea of the model is to assume that the virgin mass m_v and the char mass m_c respect the mass conservation on the domain $\Omega(t)$, when deformations occur:

$$\frac{dm_i}{dt} = 0, \quad i = v, c. \tag{3}$$

Nevertheless, intensive quantities must be used to ensure independence from system size. Thus, the model has to be written using the solid density, instead of mass. As the study domain is moving, because of macroscopic deformations - thermal expansion, swelling or shrinkage -, equations (3) need to be written with the virgin and char density, and with the macroscopic velocity of the solid \mathbf{v}^s .

$$\partial_t \rho_i + \nabla \cdot (\rho_i \mathbf{v}^s) = 0, \text{ on } \Omega(t), \quad i = v, c.$$
 (4)

Moreover, the first term in the solid mass equation (1) is classically written with the solid density, using the solid velocity. However, the pyrolysis function (2) is more complex to express in terms of density, as the virgin solid volume differs from the charred solid volume. The equation cannot be simplified by the volume that evolves over time. However, the model can alter the virgin and the char density over time using equations (4). Thus, considering a density variation of the virgin and charred solid, the pyrolysis function can be written according to the solid density. Then, the density equation can be written substituting the mass by the density in equations (1) and (2).

$$\partial_t \rho^s + \nabla \cdot (\rho^s \mathbf{v}^s) = -\Pi_\rho$$

$$= -A\rho_v \left(\frac{\rho^s - \rho_c}{\rho_v}\right)^{Na} \exp^{-\frac{Ta}{T}}.$$
(5)

Finally, solid mass conservation can be stated on the domain $\Omega(t)$ using equations (4) and equation (5). If virgin and char density remained constant, the mass conservation would be compromised. For instance, once the solid is fully charred, if there is swelling without adjusting the density, the solid mass will increase, which conflicts with the mass conservation. This phenomenon will be outlined in section 4.3.

Furthermore, solid properties are tracked by the decomposition rate ξ , using mixture law between virgin and char state, computed as follows:

$$\xi = \frac{\rho^s - \rho_v}{\rho_c - \rho_v}.\tag{6}$$

The thermal conductivity λ^s can be determined as follows:

$$\lambda^s = (1 - \xi) \,\lambda_v + \xi \lambda_c,\tag{7}$$

While the heat capacity C_p^s can be calculated as follows:

$$\rho^{s} C_{p}^{s} = (1 - \xi) \rho_{v} C_{p_{v}} + \xi \rho_{c} C_{p_{c}}. \tag{8}$$

Other mixture law may be used to model the degradation of thermal properties, without altering the overall model [8].

Moreover, during the pyrolysis of the solid, gases are produced as a result of the chemical degradation of materials. Pyrolysis gases are transported through the pore network in the charred layer and reach the surface. As a result, a source term has to be added in the gaseous mass conservation. The production term is the same pyrolysis-function (2) used in the solid mass conservation. The gas, of density ρ^g , flows through the solid at a velocity \mathbf{v}^g . The gas mass equation is expressed as a function of density on $\Omega(t)$ as follows:

$$\partial_t \rho^g + \nabla \cdot (\rho^g \mathbf{v}^g) = \Pi_\rho, \tag{9}$$

Where $\rho^g \mathbf{v}^g$ is the mass flow rate and can be written as $\dot{\mathbf{m}}^g$.

$$\dot{\mathbf{m}}^g = \rho^g \mathbf{v}^g = \rho^g \|\mathbf{v}^g\| \mathbf{D}^g, \tag{10}$$

Where \mathbf{D}^g is the gas flow direction: $\mathbf{D}^g = \frac{\mathbf{v}^g}{\|\mathbf{v}^g\|}$.

The solid considered is assumed to have very low porosity ε . Consequently, it can be considered that the solid contains no gas at the beginning and gases are released during pyrolysis reactions, excluding gas storage. Moreover, the gas density is negligible relative to the solid density, and the gas density variations are neglected. Hence, the relevant density is the solid density: $\rho = (1 - \varepsilon) \rho^s + \varepsilon \rho^g \approx \rho^s$.

Combining the solid (5) and gas (9) mass conservation, and using the previous assumption concerning the gas density, the mass flow rate equation can be written as following:

$$-\nabla \cdot \dot{\mathbf{m}}^g \approx \partial_t \rho + \nabla \cdot \rho \mathbf{v}^s = -\Pi_\rho. \tag{11}$$

Then, the energy conservation equation in the solid can be written on the moving domain $\Omega(t)$ as follows:

$$\partial_t \left(\rho^s e^s \right) + \nabla \cdot \left(\rho^s e^s \mathbf{v}^s \right) = \nabla \cdot \left(\lambda^s \nabla T \right) + S^s, \tag{12}$$

And the gas energy equation is stated as follows:

$$\partial_t (\rho^g e^g) + \nabla \cdot (\rho^g e^g \mathbf{v}^g) = \nabla \cdot (\lambda^g \nabla T) + S^g, \text{ on } \Omega(t).$$
 (13)

Where the internal energy is noted e. A heat or sink source term S can be added to the energy equation. The solid pressure is assumed to remain constant, so the solid internal energy is equal to the solid enthalpy h^s . Moreover, considering the gas density and pressure are neglected, the gas internal energy is

also equal to the gas enthalpy. Assuming the local thermal equilibrium between the solid and the gas, the temperature in both equations is the same. Combining the solid (12) and gas (13) energy conservation equations, and using the previous assumption concerning the gas density, the system energy equation can be written as following:

$$\partial_t (\rho h^s) + \nabla \cdot (\rho h^s \mathbf{v}^s) - \nabla \cdot (\lambda \nabla T) + \nabla \cdot (\dot{\mathbf{m}}^g h^g) + S = 0.$$
(14)

Where the total conductivity is set as $\lambda = \lambda^s + \lambda^g$, and the total source term is noted $S = S^s + S^g$. The gas and solid enthalpies are defined using the enthalpies of formation h_{form} :

$$h^{i} = h_{form}^{i}(T_{0}^{i}) + \int_{T_{0}^{i}}^{T} C_{p}^{i}(T')dT', \quad i = g, s.$$
 (15)

Furthermore, during the material heating and the pyrolysis process, the solid undergoes multiple deformations. In order to improve the thermal response, the volumetric deformations must be studied (excluding ablation). Initially, the solid endures swelling, then shrinkage, and can undergo thermal expansion throughout the thermal rise. A simplified 1D method had been modeled in [8]. The evolution of the size of the domain is defined by the following deformation equation:

$$\frac{1}{L}\frac{\partial L}{\partial t} = \frac{1}{L}v^s = (\alpha_v(1-\xi) + \alpha_c\xi)\frac{\partial T}{\partial t} + \frac{\eta}{m^0}\frac{\partial m}{\partial t}.$$
 (16)

Where L is the domain size, α is the coefficient of thermal expansion, η is a deformation coefficient and $m \approx m^s$. In this way, swelling and shrinkage can be taken into account according to the sign of η . This first simplified model is 1D and can be extended to 2D using the same equation with the length in the second direction. However, the drawback is to calibrate the deformation coefficients.

3. Numerical resolution

3.1. Overview of a time iteration resolution

The SPA²RC code (Simulation of Pyrolysis and Ablation using Adaptative gRid with respect to Conservation) is a research tool designed to simulate the solid thermal response, considering pyrolysis and deformations, and using mesh adaptation. This study code is a 2D finite volume code, using a Cartesian mesh. The initial mesh can be uniform, or refined near the wall using a linear or beta law. Time discretization is performed using implicit Euler scheme. Mesh motion and terms of equations (5) and (14) can be solved explicitly or implicitly.

During a time iteration, three steps must be resolved. First, a new mesh is computed, according to a wall recession due to ablation, which is given as input, or according to a mesh adaptation, depending on temperature and density gradients. Once the new mesh is computed, the virgin and char density (4) must be calculated based on the updated mesh. Second, thermal resolution is carried out to obtain the thermal quantities at the intermediate time, denoted with a superscript n+1-, but which have not yet experienced deformations. The density (5), the mass flow rate (11) and the temperature (14) are determined using one resolution described in section 3.2. Since thermal properties (conductivity and heat capacity) are temperature-dependent, the energy equation is non-linear and requires an iterative solver to preserve the correlation between temperature and thermal properties. The chosen solver is a biconjugate gradient (BiCG). Moreover, thermal properties are also updated as a function of the pyrolysis advancement rate (6). The direction of pyrolysis gases is given as input. Thirdly, an additional mesh movement is applied to take account of the solid deformations. The Henderson's equation (16) is computed in steady-state, using the input deformation coefficients. At this step, the solid thermal properties have been computed on the solid domain which has not been deformed yet. Therefore, a conservative projection must be carried out between the adapted and ablated domain, where the quantities are computed, and the deformed domain, which has increased due to swelling or reduced due to shrinkage. In other words, on each cell i of the mesh, conservation laws are applied to obtain the thermal quantities at the time n+1. Since

deformations were computed in steady-state, the mass and the energy on each cell i of volume Ω_i must be conserved. Thus, the following equations must be resolved in each cell of the mesh:

$$m_i^{n+1} = m_i^{n+1-} \Leftrightarrow \rho_i^{n+1} = \frac{\Omega_i^{n+1-}}{\Omega_i^{n+1}} \rho_i^{n+1-},$$
 (17)

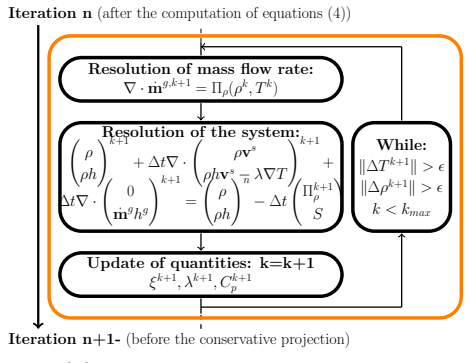
$$m_i^{n+1}h_i^{n+1} = m_i^{n+1-}h_i^{n+1-} \Leftrightarrow h_i^{n+1} = h_i^{n+1-}.$$
 (18)

Assuming that the local heat capacity is not affected by the solid deformations, the energy conservation leads to the temperature conservation in each cell.

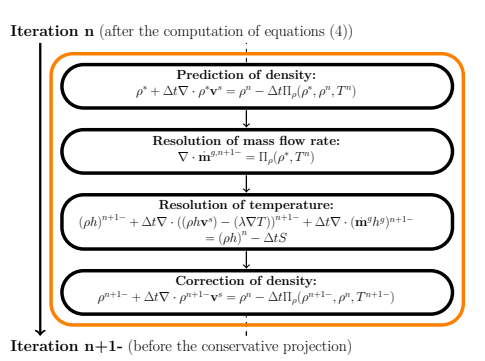
3.2. Pyrolysis-thermal resolution method

Once the model is established and the equations are discretized, the next step is to choose the appropriate resolution method to solve equations (5), (11) and (14). Density and temperature are correlated variables in the system of equations. This means that both quantities can be solved simultaneously, or split into independent sub-resolution. These two methods are investigated.

The first resolution method is a Newton's method (N). The aim is to solve density and temperature at the same time, keeping the correlation between the two quantities. This method, described in Figure 2(a), can be used to solve non-linear systems like this one. ϵ is the Newton's tolerance and Δt is the time-step. A vector U, containing the density and the temperature, is assumed to be the unknown for the system. In a Newton iteration k, the gas flow equation (11) is solved first. Then, using the updated mass gas flow, the system of equations (5), (14) is resolved, and the relevant quantities are subsequently updated. As long as convergence is not obtained $\|\Delta U^{k+1}\| = \|U^{k+1} - U^k\| > \epsilon$ or the maximum number of Newton iterations is not exceeded $k < k^{max}$, the computation is repeated which is time-consuming.



(a) Newton resolution method



(b) Prediction-correction resolution method

Fig 2. Pyrolysis-thermal coupling resolution methods.

One idea to reduce the resolution time is to dissociate the resolution of density and temperature. The first approach, called direct resolution (D), separately resolves density and temperature. Equation (5) is computed first, followed by equation (14) in each time iteration. An other method is a prediction-correction method (PC). The goal of this method is to recover the density-temperature correlation, which was broken by the direct resolution. First, the mass conservation equation (5) is solved to get a prediction of the density, noted ρ^* , with the temperature at the current time. Then, the energy equation (14) is solved with the predicted density to obtain the temperature value. Finally, a density correction is computed by solving the same mass conservation equation (5) with the temperature at the next time to obtain the density. The three resolution steps are described in Figure 2(b). The prediction-correction method splits the resolution of the two physical quantities, by correcting density only. However, without a temperature correction the question of preserving non-linearities may arise. Therefore, the prediction-correction approach was enhanced by incorporating a temperature correction and iterating the process, looping over the prediction and the correction of both density and temperature until convergence or until

the maximum number of iterations has been reached. In this way, the correlation between temperature and density is preserved. This is an iterative prediction-correction method (IPC).

4. Results and validation

4.1. Conservative methods

One of the aims of this work is to analyze the impact of resolution on mass and energy conservation addressing a pyrolysis problem. For this purpose, a test case has been created, which is illustrated in Figure 3. A square of pyrolysable materials is separated into two parts along the vertical. At the initial time, the solid is composed of a material with virgin properties at the bottom of the square with an initial temperature T_0 and pyrolyzed properties at the top with a temperature ten times higher than T_0 . Zero fluxes are assumed at all boundaries. The virgin material at the bottom will be heated by the warmer material, and will pyrolyze, which means its physical properties will match those of the top material. Pyrolysis gases flow upwards and are zero on the bottom edge condition. The temperature will homogenize across the solid. Furthermore, a deformation law is solved (16). Thus, the solid will experience a swelling of about 50% by the end of the simulation.

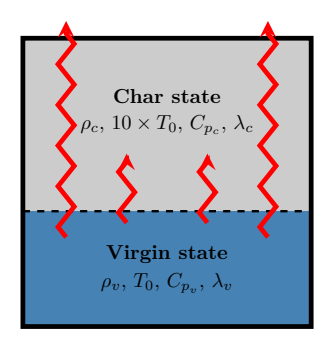


Fig 3. Conservative test case.

The mesh is composed of 20 vertical and 5 horizontal cells. The time step is 0.1s and remains constant. The initial temperature is 293 K. The tolerance for the Newton is 10^{-12} , with a maximum of 200 iterations, and that of the BiCG solver is 10^{-16} . A diagonal preconditioner is used.

Pyrolysis results in a mass loss, which is converted into escaping gases at the top of the domain. Therefore, mass conservation must be computed taking account escaping gases at each time step. The conservation of mass is demonstrated using the following relationship:

$$\Delta m_{norm}^n = \frac{|m^n + m_{out}^n - m^0|}{m^0} \tag{19}$$

Where the total solid mass is m^n and the initial mass is m^0 . The subscript *out* describes the surface where pyrolysis gases are released, the mass loss is computed as follows:

$$m_{out}^n = \int_{out} \int_{t^0}^{t^n} \dot{m}^g \mathbf{D}^g \cdot \mathbf{n}_{out} dt dx.$$
 (20)

The same approach must be used to compute energy conservation, ΔE_{norm}^n , considering the energy loss convected by the escaping gases at the top of the domain, $h^g \dot{m}^g \mathbf{D}^g \cdot \mathbf{n}_{out}$.

The solid is fully charred after 30 seconds, while the swelling occurs throughout the simulation. It can be highlighted that the direct resolution is not mass conservative but energy conservative, as shown in Figures 4. The density-temperature splitting used during resolution introduces a mass conservation error, which could be lower reducing the time-step. The prediction-correction resolution is neither mass conservative as shown in Figure 4(a) nor energy conservative as shown in Figure 4(b). The density correction attempts to recover the initial shift of the mass conservation, but introduces instability on the energy conservation. The two methods allowing mass and energy conservation are the iterative

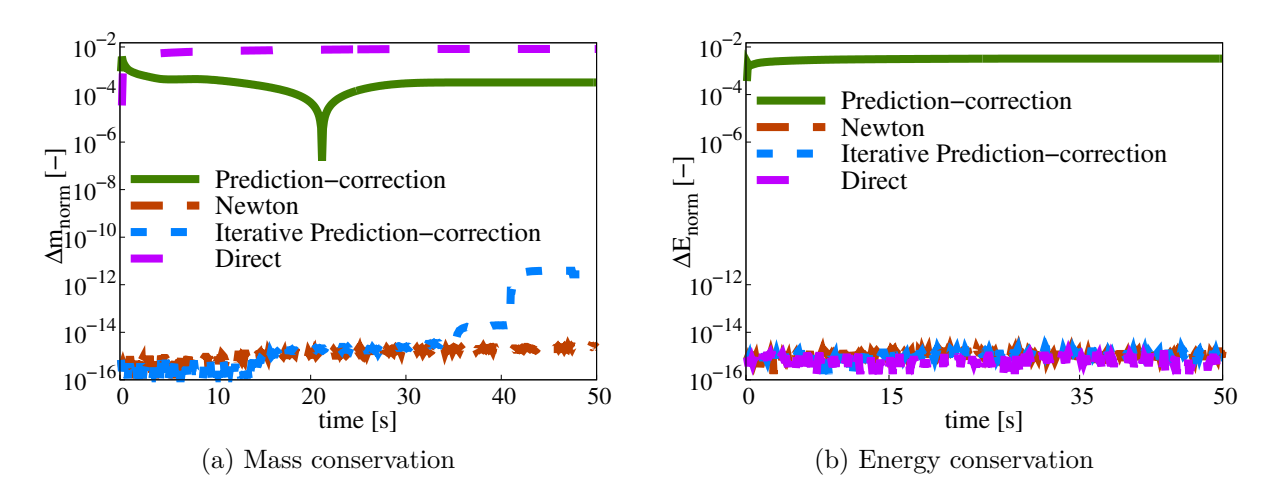


Fig 4. Conservation for different resolution methods.

		Iterative	
Method	Prediction-	Prediction-	Newton
	correction	correction	
Time/Time(D)	1.01	17.09	3.96

Table 1. Computation time

methods, which are consistent with the given tolerance. Computation times normalized by the direct method computation time are given in the Table 1. The Newton resolution is less time-consuming than the iterative prediction-correction method. Thus, the Newton resolution is selected for the following cases.

4.2. Ablation Workshop Test Case [10]

This one-dimensional test case was presented at the 4th Ablation Workshop [10]. The sample studied is 0.05 meters of the Theoretical Ablative Composite for Open Testing (TACOT), which is porous at 80% and composed of 10% of carbon fibers and of 10% of phenolic resin. The sample is warmed at 1644~K on the top for 60 seconds while adiabatic boundary condition is used on the bottom of the sample. The initial temperature is 298~K. Even if the model is made for less porous materials, it can be adapted to represent the TACOT's material response, which is a classic benchmark of literature.

Material thermal response computed by SPA 2 RC fits well with the one of FIAT and PATO, as shown in Figure 5(a) for the temperature within the solid and in Figure 5(b) for the density. This ensures that the code can accurately describe a thermal response of a solid. Furthermore, it is worth noting that the Newton resolution results are not significantly different from the direct resolution results. In fact, the maximum temperature difference between the two resolutions is 13.6K, which represents less than 1.5%.

4.3. Henderson's 1985 test case [7]

The model including deformation is validated against Henderson's 1985 experimental test case [7], which investigates the thermal decomposition of a composite material. The composite material studied is H41N, which consists of 60.5% of glass-fiber and 39.5% phenolic resin by volume. The sample is a 0.03 meters H41N block, exposed to a constant heat flux of 279.7 $kW.m^{-2}$ for 800 seconds. The initial block temperature is 297.15 K and its sides are thermally insulated. In order to monitor the temperature profile during the experiment, thermocouples (TC) are inserted into the material at depths of 1, 5, 10, and 29 mm from the heated surface, as shown in Figure 6. SPA²RC is compared with the Henderson's

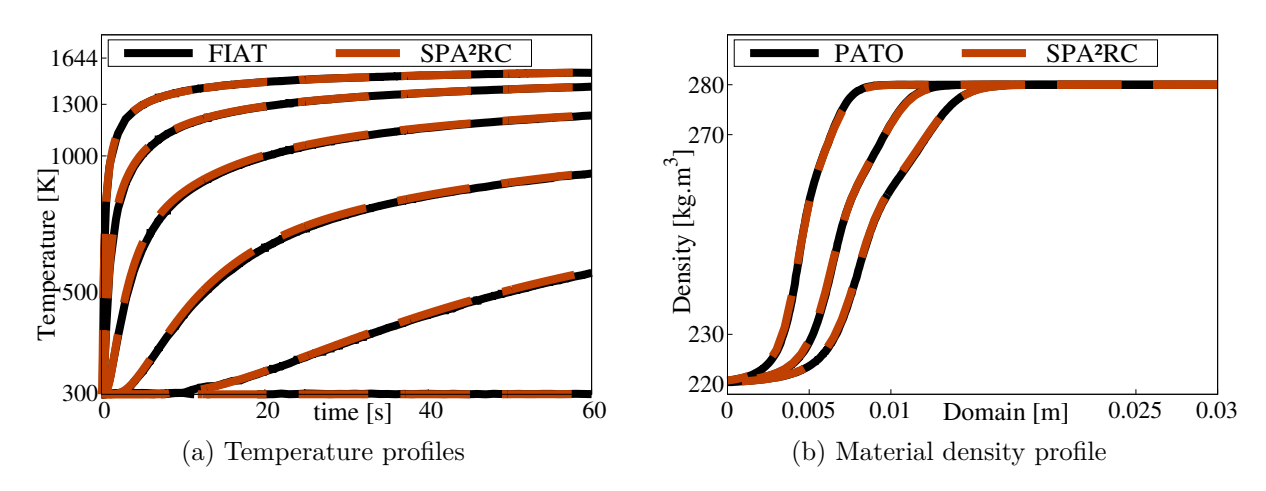


Fig 5. Comparison between FIAT/PATO and SPA²RC.

1987 simulation [8] performed with a type 2 model. Henderson introduced a rate of decomposition in the energy equation, driven by the heat of decomposition Q, as a source term $S = Q \frac{\partial \rho}{\partial t}$.

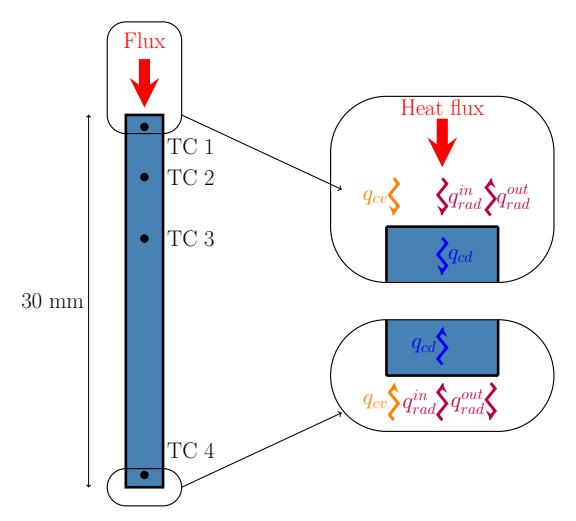


Fig 6. Reference case study.

The material properties, provided by Henderson [7], are listed in SI units in Table 2. Henderson underlined that the specific heat capacity of the material was measured up to 1000~K and the thermal conductivity was measured up to 1120~K. In his thesis, Biasi [3] recommended thresholding the thermal conductivities and the heat capacities at 1000~K. Furthermore, the parameters used for the Arrhenius laws and for the domain deformation are those determined by Henderson [8]. The coefficients depend on the density. Thus, the coefficients are adjusted, enabling the model to predict the temperature for several experimentally performed heating rates.

For boundary conditions, zero fluxes are considered on the sides of the bar, and radiative and convection-diffusion fluxes are considered at the top and bottom of the plate. In addition, the top part is heated by the constant flux of $279.7 \ kW.m^{-2}$. Useful values for boundary conditions are described in the Table 3, based on data from [16].

First, temperature at the thermocouples is compared with the Henderson experiment [7] in Figure 7(a). SPA²RC and Henderson simulations yield broadly similar results. These results match roughly those

Range Property Value 1810 ρ_v 1440 ρ_c $0.73 + 2.76 \times 10^{-4}T$ T < 1000 λ_v $0.31 + 4.26 \times 10^{-3}T - 8.43$ λ_c $\times 10^{-6}T^2 + 5.32 \times 10^{-9}T^3$ $T \leq 1000$ C_{pv} $791.23 + 1.09 \times T$ $T \le 1000$ $601.33 + 1.02 \times T$ $T \leq 1000$ C_{pp} Q 2.34×10^{5} C_p^g 9630

Table 2. H41N Properties (SI units)

Table 3. Boundary condition coefficients

Property	Unit	Value
$\overline{h_{conv}}$	$W.m^{-2}.K^{-1}$	25
σ	$W.m^{-2}.K^{-4}$	5.73×10^{-8}
ϵ_s	_	0.9
T_{ext}	K	297.15

obtained from the experiment. The discrepancies may be explained by the material properties, such as heat capacities or conductivities, which are difficult to measure. The law of mixtures model for properties could be improved, if properties could be determined on materials undergoing pyrolysis. Furthermore, the discrepancies can be justify by an oversimplified model. In Figure 7(b), the mass flow rate in the domain at 50, 200 and 800 seconds are compared between the two codes. These results confirm that accurate gas modeling is not essential in 1D. Without using Darcy' law, without modeling pressure and neglecting gas density, mass flow rate is still well computed.

Then, the swelling is studied. At the end of the simulation, SPA²RC computed a H41N block swelling of around 8% and Henderson computed a swelling of approximately 10% in 1987 [8] and 7% in 1991 [6]. Moreover, two pyrolysis models implemented in the SPA²RC code were compared. First, the model described in section 2.2 is displayed in orange in Figures 8. A more traditional pyrolysis model where virgin and char density remain constant all over the simulation is displayed in green in Figures 8. Henderson model, computed using virgin and char mass instead of density, is also displayed in black. Mass in the domain at 50, 200 and 800 seconds is shown in Figure 8(a). As expected, the mass results between the current model and the Henderson model are very close. However, a constant virgin and char density pyrolysis model is not mass conservative. Indeed, when swelling is taken into account, it can be seen that mass is generated during the simulation before being lost due to pyrolysis, which is physically impossible. Next, density in the domain is analyzed in Figure 8(b). Since constant virgin and char density pyrolysis model imposes an initial and final density, regardless of swelling, the density will remain within the fixed limits given as input. Nevertheless, the current model allows density limits to be adjusted by taking swelling into account. In the end, the final char density at the top of the domain is lower than the char density imposed at the input. Similarly, the final virgin density at the bottom of the domain is lower than the initial virgin density due to the swelling. In this way, the pyrolysis model taking deformation into account is validated, and it should be underlined that virgin and char density must be altered to respect conservation of mass.

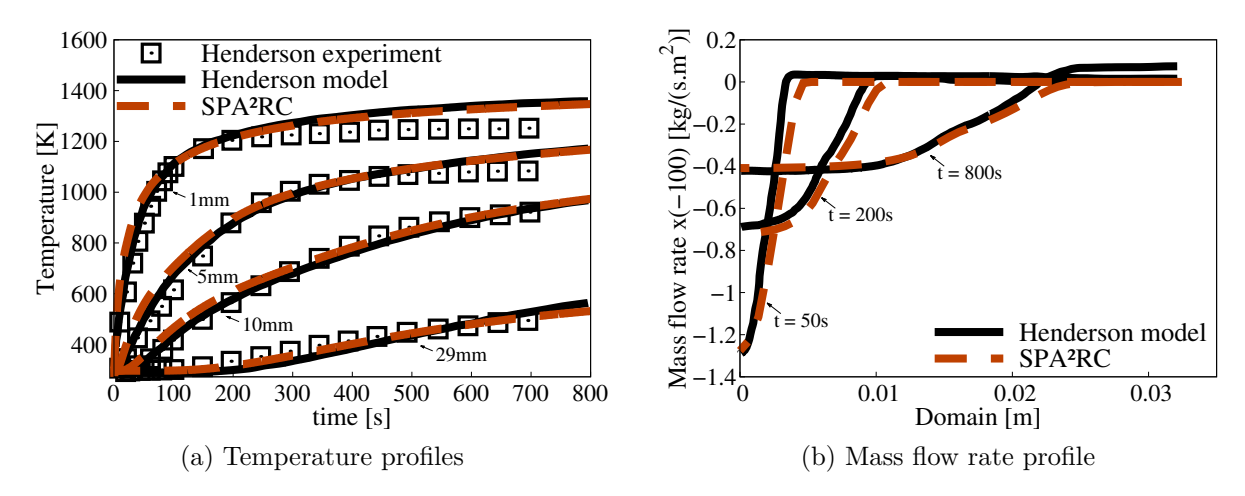


Fig 7. Comparison of SPA²RC and Henderson results [8].

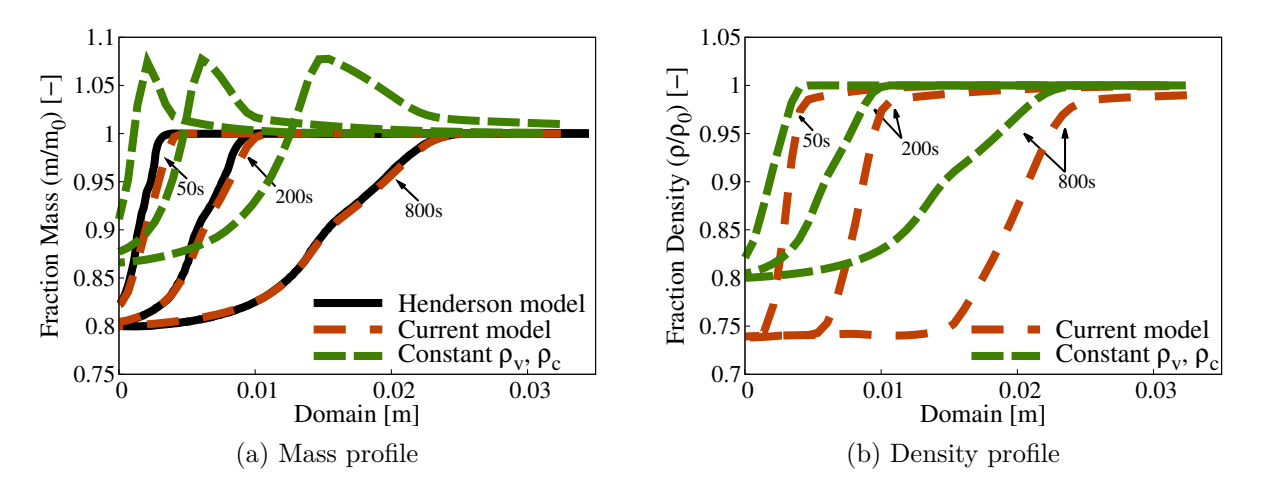


Fig 8. Comparison of the constant virgin and char density model with the new model, considering the swelling.

5. Conclusions

The conservation of physical properties was a key concern of the study. On the one hand, this focus had highlighted the importance of the pyrolysis-thermal resolution. While the different resolution methods do not significantly alter the temperature results, a strong coupling between density and temperature resolution is necessary to conserve mass and energy during simulations. These conservation properties require a higher computational cost and result in limited improvement. Therefore, a trade-off between computation time and conservation must be chosen. On the other hand, this work revealed the benefits of using a variable virgin and char density model during solid deformation. Indeed, in order to be physically consistent, virgin and char density must be adjusted, according to the mass conservation.

The pyrolysis model could be further enhanced by considering Darcy's law or by using several Arrhenius non-parallel laws. Besides, the deformation law could be improved by computing the momentum conservation law and the internal stress. Finally, 2D cases need to be validated with this model.

References

[1] C.E. Anderson Jr et D.K. Wauters: A thermodynamic heat transfer model for intumescent systems. *International Journal of Engineering Science*, 22(7):881–889, 1984.

- [2] C.H. Bamford, J. Crank et D.H. Malan: The combustion of wood, part i. *In Mathematical Proceedings of the Cambridge Philosophical Society*, volume 42, pages 166–182. Cambridge University Press, 1946.
- [3] V. Biasi: Modélisation thermique de la dégradation d'un matériau composite soumis au feu. Thèse de doctorat, Institut superieur de l'aeronautique et de l'espace, 2014.
- [4] Y.-K. Chen et F.S. Milos: Ablation and thermal response program for spacecraft heatshield analysis. *Journal of Spacecraft and Rockets*, 36(3):475–483, 1999.
- [5] J.F. EPHERRE et L. LABORDE: Pyrolysis of carbon phenolic composites. In Fourth International Symposium Atmospheric Reentry Vehicles and Systems, 2005.
- [6] J. FLORIO JR, J.B. HENDERSON, F.L. TEST et R. HARIHARAN: A study of the effects of the assumption of local-thermal equilibrium on the overall thermally-induced response of a decomposing, glass-filled polymer composite. *International Journal of Heat and Mass Transfer*, 34(1):135–147, 1991.
- [7] J.B. HENDERSON, J.A. WIEBELT et M.R. TANT: A model for the thermal response of polymer composite materials with experimental verification. *Journal of composite materials*, 19(6):579–595, 1985.
- [8] J.B. HENDERSON et T.E. WIECEK: A mathematical model to predict the thermal response of decomposing, expanding polymer composites. *Journal of composite materials*, 21(4):373–393, 1987.
- [9] K. Kratsch, L. Hearne et H. McChesney: Thermal performance of heat shield composites during planetary entry. *In Engineering Problems of Manned Interplanetary Exploration*, page 1515. 1963.
- [10] J. LACHAUD, A. MARTIN, I. COZMUTA et B. LAUB: Presentation of the 2011 ablation test case. 2011.
- [11] J. LACHAUD, T. VAN EEKELEN, J.B. SCOGGINS, T.E. MAGIN et N.N. MANSOUR: Detailed chemical equilibrium model for porous ablative materials. *International Journal of Heat and Mass Transfer*, 90:1034–1045, 2015.
- [12] F. LAHOUZE, W. JOMAA, C. MÉTAYER, M. MEYER, F. PANERAI et J. LACHAUD: Pyromechanics: A solid mechanics approach to deformation during pyrolysis. *Fuel*, 390:134557, 2025.
- [13] C.B. MOYER et R.A. RINDAL: An analysis of the coupled chemically reacting boundary layer and charring ablator. part 2-finite difference solution for the in-depth response of charring materials considering surface chemical and energy balances. Rapport technique, NASA, 1968.
- [14] J.E.J. STAGGS, R.J. CREWE et R. BUTLER: A theoretical and experimental investigation of intumescent behaviour in protective coatings for structural steel. *Chemical Engineering Science*, 71:239–251, 2012.
- [15] F. Torres-Herrador, J. Coheur, F. Panerai, T.E. Magin, M. Arnst, N.N. Mansour et J. Blondeau: Competitive kinetic model for the pyrolysis of the phenolic impregnated carbon ablator. *Aerospace Science and Technology*, 100:105784, 2020.
- [16] Y. Zhang, D. Behera et E. Madenci: Peridynamic modeling of thermal response and cracking in charring materials due to ablation. *Engineering with Computers*, 40(1):343–365, 2024.